Progress of Theoretical Physics, Vol. 89, No. 2, February 1993

A Numerical Study of Galaxy Formation and the Large Scale Structure of the Universe

Kazuyuki YAMASHITA

Department of Physics, Kyoto University, Kyoto 606-01

(Received November 24, 1992)

We investigate the thermodynamical and hydrodynamical effects on the structure formation on scales of $20h^{-1}$ Mpc in the Einstein de-Sitter universe by three-dimensional numerical simulation. Calculations involve cosmological expansion, self-gravity, hydrodynamics, and cooling processes with $100\times100\times100$ mesh cells and the same number of CDM particles. Galactic bursts out of young galaxies as a heat input are parametrically taken into account. We find that the thermodynamics of the intergalactic medium plays an important role in formation of galaxies, the rate of galaxy formation depends on the amount of the energy burst from galaxies, and that the critical energy scale to affect the structure of the universe is 10^{57-59} erg.

§ 1. Introduction

Recent observations reveal the large scale structure of the universe. The feature of the "Great Wall" was found from the CfA survey.[1] The periodic structure was discovered by the pencil beam survey[2] and it has been clarified, from the observations of the other direction, that it may be the cellular structure. As for the thermodynamical properties of the universe, observations of X-ray have clarified the properties of intracluster gaseous matter and active galactic nuclei. The evolution of the observed luminosity function of X-ray clusters is an important evidence that the temperature and the density of the intracluster gas evolve due to the gravity of clusters and/or the activity of galaxies. The HI optical depth[3] of the intergalactic medium (IGM) is estimated from QSOs spectra. Then hydrogen in the IGM is found to be highly ionized at redshift $z<4$,[4] which does not agree with model prediction of structure formation as described later.

On the other hand theoretical views on the structure of the universe have mainly pointed at the distribution of galaxies, and many researchers have carried out cosmological N-body simulations.[5)~8)] However galaxy formation rules based on crowdedness of collisionless particles, such as identifying particles at high density peaks with "galaxies", are less physical meaning. A galaxy must be constructed from the gaseous matter. The thermodynamical effect such that thermal pressure plays an important role for this process since it may prevent fluid from collapsing gravitationally. Actually, when the system of the scale length R has the temperature T, and the gravitational mass density ρ_t, the ratio of the thermal energy to the gravitational energy is written as $6.9\times10^{-6}(T/1\mathrm{K})(R/1h^{-1}\mathrm{Mpc})^{-2}(\rho_{\mathrm{cr}}/\rho_t)$, where ρ_{cr} is the critical density of the universe. This ratio becomes larger than unity locally for the system to be considered here. The N-body method does not include the thermodynamical effect properly and may lead to overestimate the crowdedness of galaxies in their analyses. Thus that method may be too simple to simulate the real situation of the large scale structure of the universe. Development in observations

described above requires more realistic model calculations.

Recently the hydrodynamical simulations for the universe were carried out by several authors.[9)~13)] These works take galaxy formation from baryonic fluid and the cooling processes into account and then the reality is increased. However we would point out the following lack in their calculations. As pointed out by Cen et al.,[11)] the number of mesh cells used in Ryu et al.[10)] is small, 32^3, and the spatial resolution is insufficient. Because thermodynamical criteria are not included in their galaxy formation rule, too many galaxies may be formed at late epoch in the universe and the IGM may be heated too high. Furthermore the energy of a galactic burst of 10^{60} erg adopted by Ryu et al.[10)] seems to be too large since it much exceeds the binding energy of a galaxy with $10^9 M_\odot$, $\sim 10^{56}$ erg, corresponding to mass scale of galaxies formed in their simulation, according to the empirical study by Saito.[14)] Although calculation of the cooling processes in Cen et al.[11)~13)] are advanced, galaxy formation is resolved poorly in time and heating mechanism such as galactic bursts used by Ryu et al.[10)] is not taken into account. This incompletion should be considered.

The problem considered here has many "parameters" such as the cosmological parameters, the initial spectra of density perturbation, the ratio of baryon and dark matter, the criteria of galaxy formation, and an activity of galaxies. Here we investigate the effects of an activity of galaxies and galaxy formation on the properties of the intergalactic medium, galaxies, and dark matter by three dimensional hydrodynamical simulation. In particular the thermodynamical history of the IGM and the spatial distributions of the IGM, galaxies, and dark matter are well discussed.

This paper is organized as follows. The equations and the methods of calculation are given in § 2. In § 3, we show the results of our simulations. Finally § 4 is devoted to the conclusions and discussion.

§ 2. Formulations

The system we consider here includes expansion of the universe, local gravity and hydrodynamics. The hydrodynamical properties of baryonic matter depend on the thermal processes such as heating and cooling. We describe equations for this system and give methods to solve them.

2.1. *Cosmological expansion*

Cosmological expansion in the Friedmann-Robertson-Walker model is given by

$$\frac{da}{dt}=H_0 a(\Omega_0 a^{-3}+\lambda_0-(\Omega_0+\lambda_0-1)a^{-2})^{1/2}, \tag{1}$$

where a, t, H_0, Ω_0 and λ_0 are the scale factor, the cosmological proper time, the present-day Hubble constant, the density parameter, and the cosmological constant normalized by $3H_0^2$, respectively. We adopt the cosmological parameters, for simplicity, as $\Omega_0=1$, $\lambda_0=0$ and $h=H_0/(100\ \mathrm{km/sec/Mpc})=1$ in our calculations.

2.2. *Gravity*

We do not consider any strong gravitational sources, much early epoch of the

universe, and the horizon scale of the universe. Then we treat the local gravity which is given by Newtonian force as follows,

$$\nabla^2\phi=4\pi G(\rho-\langle\rho\rangle)/a\,, \tag{2}$$

where ϕ and ρ are the proper peculiar gravitational potential and the comoving density of matter which consists of dark matter, galaxies and baryonic matter, and $\langle\rangle$ denotes the spatial average. As for the method of numerical calculation, we adopt the cloud-in-cell (CIC) method,[15] in order that the mass of dark matter and galaxies is assigned into the density. Equation (2) is solved using FFT since the periodic boundary condition is imposed. We should note that the resolution of the force calculated by the CIC scheme is limited above 2 meshes.

2.3. *Equations of motion of particles*

Dark matter and galaxies are treated as particles. Whole of dark matter particles have the same mass, while galactic particles have different mass according to our formation rule described later. The motion of each particle is given by

$$\frac{dv_i}{dt}+\frac{\dot{a}}{a}v_i=-\frac{1}{a}\frac{\partial\phi}{\partial x_i}\,, \tag{3}$$

$$\frac{dx_i}{dt}=\frac{1}{a}v_i\,, \tag{4}$$

where v_i and x_i are the proper peculiar velocity of particles and the comoving coordinates of particles, respectively, with $i=1, 2, 3$. We use the time-centered-leap-frog method[10),15] to integrate Eqs. (3) and (4) numerically. The part of solving gravity has been checked with the Layzer-Irvine test. Then we have found that the accuracy of energy conservation is greater than 99%.

2.4. *Hydrodynamical equations*

The intergalactic baryonic matter follows the hydrodynamic equations, which are primarily conservative form and couple to the cosmic expansion, Newtonian gravity, and thermal processes. The mass conservation equation is

$$\frac{\partial\rho_{\rm b}}{\partial t}+\frac{1}{a}\frac{\partial\rho_{\rm b}u_k}{\partial x_k}=-\delta_{\rm gal}\,. \tag{5}$$

The Euler equations are

$$\frac{\partial\rho_{\rm b}u_i}{\partial t}+\frac{1}{a}\frac{\partial}{\partial x_k}[\rho_{\rm b}u_iu_k+p\delta_{ik}]=-\frac{\dot{a}}{a}\rho_{\rm b}u_i-\frac{1}{a}\rho_{\rm b}\frac{\partial\phi}{\partial x_i}-u_i\delta_{\rm gal}\,. \tag{6}$$

The energy "conservation" equation is

$$\frac{\partial E}{\partial t}+\frac{1}{a}\frac{\partial}{\partial x_k}[(E+p)u_k]=-\frac{2\dot{a}}{a}E-\frac{1}{a}\rho_{\rm b}u_k\frac{\partial\phi}{\partial x_k}-\Lambda_{\rm cool}+\Lambda_{\rm heat}-\Lambda_{\rm loss}\,. \tag{7}$$

Here we denote $\rho_{\rm b}$, u_i, x_k, $\Lambda_{\rm heat}$ and $\Lambda_{\rm cool}$, respectively, as the comoving density of the IGM, the proper peculiar velocity of the IGM, the comoving coordinates, the rate of heating burst from galaxies, the cooling/heating rate including bremsstrahlung cool-

ing, recombination cooling, dielectronic recombination cooling, ionization cooling, line cooling, which are hereafter called "collisional" cooling and Compton cooling. The thermal pressure and the comoving total energy density, that is the peculiar kinetic energy density plus the thermal energy density of the IGM, are denoted as p and E, respectively. When a galaxy is formed in a cell, as described in § 2.6, the conservation is violated by $\delta_{\rm gal}$ and $\Lambda_{\rm loss}$ which are the rate of the mass transformed into galaxies, and the rate of energy loss due to galaxy formation, respectively. We adopt the specific heats 5/3.

These equations are integrated by the Roe method which does not need an artificial viscosity and is a well conserving scheme.[16] We adopt first order of accuracy because of avoiding occurrence of negative pressure, which will be improved. Since the resolution of the CIC scheme is limited above 2 meshes, calculation of higher order of accuracy is less needed at this time. Time step is determined by the minimum of Hubble time scale, free-fall time scale, cooling time scale, and hydrodynamical time scale which is (length of one mesh)/$v_{\rm sound}$ and then explicit Euler advancing is carried out. The hydrodynamical part of the code has checked with the point explosion excluding cosmological expansion and any source terms, which is known as the Sedov solution. We have found that the total energy is conserved in 99% accuracy and the shock detection can be done in 2 meshes.

2.5. *Cooling rate*

As for the cooling rate of $\Lambda_{\rm cool}$ in Eq. (7) we conventionally use the table given by Kang and Shapiro,[17] which is based on the equilibrium cooling of a primordial hydrogen and helium gas. Here we should note that full ionization of H and He is satisfied at temperature $T \gtrsim 10^5$ K and that the "collisional" cooling is effective at $T \sim 10^{4-5}$ K, according to Kang and Shapiro.[17] These temperatures are important to understand the behavior of the matter.

2.6. *Galaxy formation and heating by galactic bursts*

Criteria of galaxy formation are imposed for cubic neighboring $8(=2^3)$ cells because of the limit of the resolution in our code to be the 2 meshes. Of course 27 $(=3^3)$ cells or more cells are preferable to compare with the observations but the CPU time of numerical calculation is limited. So we investigate what we can do with the neighboring mesh cells here. We adopt the following rule for galaxy formation. If the neighboring eight cells satisfy whole of five conditions as follows, (i) $M_{\rm IGM} \geq M_{\rm Jeans}$, occurrence of gravitational instability, (ii) $\nabla \boldsymbol{u} < 0$, collapsing phase, (iii) $M_{\rm tot} \geq \alpha_1 \langle M_{\rm tot} \rangle$, (iv) $M_{\rm IGM} \geq \alpha_2 \langle M_{\rm IGM} \rangle$, the meanings of (iii) and (iv) are described later, and (v) $T < 2 \times 10^5$ K, cooling to be effective, then a "galaxy" is forced to be formed at the center of mass of the eight cells. Here $M_{\rm IGM}$, $M_{\rm tot}$, $M_{\rm Jeans}$ and $\boldsymbol{u}$ are the mass of the IGM, the mass of baryon and dark matter, the Jeans mass, and the velocity of the IGM, respectively. A formed galaxy is treated as a particle that its mass is 90%, which is unknown in reality, a parameter fixed here, of mass of the neighboring eight cells and that its initial velocity is sum of the velocities of the eight cells. Galaxies move according to Eqs. (3) and (4) as well as dark matter particles. The conditions (iii) and (iv) seem to be somewhat artificial while they are well known as "biased

galaxy formation". The reasons of adopting these conditions here are the following. The condition (iii) means that galaxies should not be formed at the beginning of calculation. The condition (iv) is needed in order not to form galaxies at the same point sequentially. The coefficients α_1 and α_2 are just parameters, and then we here adopt $\alpha_1=3$ and $\alpha_2=1$ but other choices are also possible. When a galaxy is formed, for the eight cells the 90% of mass is subtracted, the velocity is kept, and the thermal energy is reduced to be the amount of 10% according to subtraction of mass so that the energy per a gas particle should be kept. Although the mass transformed into a galaxy is an unknown parameter, here we consider a single value of 90% which is used in Ryu et al.[10] The change of this parameter would affect the history of the IGM.

As for an activity of young galaxies, we suppose that the energy of $\epsilon M/10^9 M_\odot$ erg is emitted from a galaxy into the neighboring eight cells during 10^8 years after it is formed, where M is the mass of the galaxy and ϵ is a parameter concerned with the explosion energy. We consider three cases, $\epsilon=0$, 5×10^{56} and 5×10^{59}. The energy of the second case corresponds to the binding energy of a galaxy when its mass is $\sim10^9 M_\odot$, according to Saito.[14] The energy of the third case much exceeds the binding energy, so the galaxy must be disrupted. Therefore it seems to be unrealistic while the sizable energy input 10^{60} erg per one galaxy with $10^9 M_\odot$ is adopted by Ryu et al.[10]

This procedure of galaxy formation and bursts described here is carried out at every time step.

2.7. *Initial conditions*

Initially, at $a=0.05$ in our normalization which $a=1$ at the present time, the Zel'dovich displacements[15] for dark matter particles are carried out using the Zel'dovich-CDM spectra with the transfer function according to Bardeen et al.[18] and the same distribution for baryonic fluid is imposed. Their amplitudes are determined by the present-day amplitude of the two point correlation function at $r=5h^{-1}$ Mpc to be $O(1)$. The amount of baryon and dark matter are $\Omega_b=0.1$ and $\Omega_d=0.9$, respectively. Baryonic matter consists of 90% hydrogen and 10% helium by number. Calculations are carried out during $a=0.05-1.0$ and the box size of all simulations are fixed to be $20h^{-1}$ Mpc. The number of mesh cells is $100\times100\times100$ and the number of particles of dark matter is the same.

§ 3. Results

We totally calculate four cases. One is, the model (A), that galaxies are not formed. The other three are the model (B) $\epsilon=0$, the model (C) $\epsilon=5\times10^{56}$ and the model (D) $\epsilon=5\times10^{59}$, as described in § 2.6.

3.1. *History of the density and the temperature*

We present the history of the density fluctuation of the dark matter and the IGM, and that of temperature of the IGM in Figs. 1(a)~(d), which correspond to the models, (A)~(D), respectively. We also show the history of the cooling/heating rate in Figs. 2(a)~(d). The galaxy formation rate is shown in Fig. 3 for the models (B)~(D).

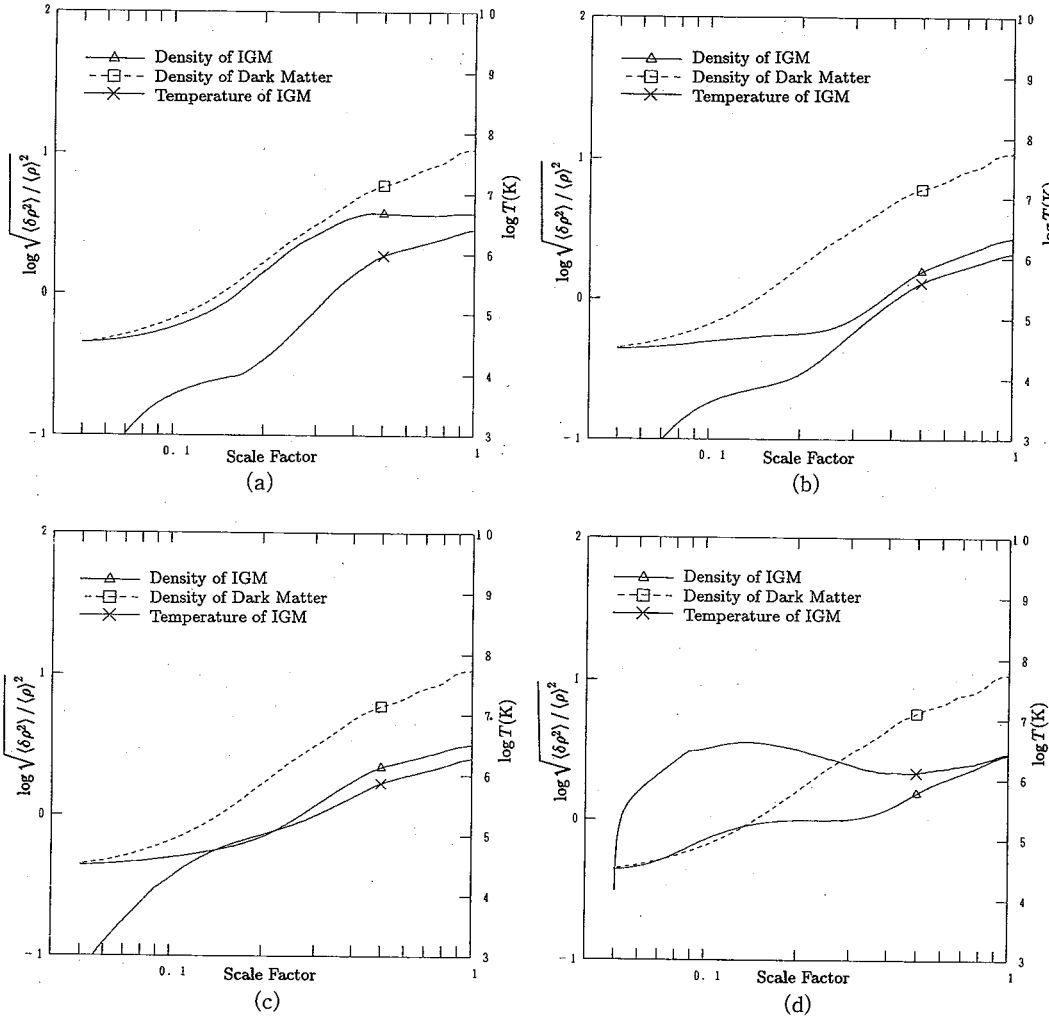

Fig. 1. The history of the density fluctuation of the dark matter and the IGM and the temperature of the IGM. The temperature is shown in units of Kelvin. (a)~(d) correspond to the models (A)~(D), respectively.

For the model (A), the case of no-formation of galaxies, the density fluctuation of the IGM follows that of the dark matter when $a \lesssim 0.4$ and it is bounced when $a \gtrsim 0.4$. This is because the "collisional" cooling which is important at high density regions, becomes ineffective as the universe expands and then the temperature at high density regions becomes so high that the pressure prevents such the region from collapsing gravitationally. The gravitational heating is always important in the system totally and it tries to heat IGM up to 10^7 K in the age of the universe. The rate of "collisional" cooling which is proportional to the square of the density of IGM is initially smaller than that of adiabatic cooling. While the rate of "collisional" cooling becomes large as the IGM is clustered, it decreases with expansion of the

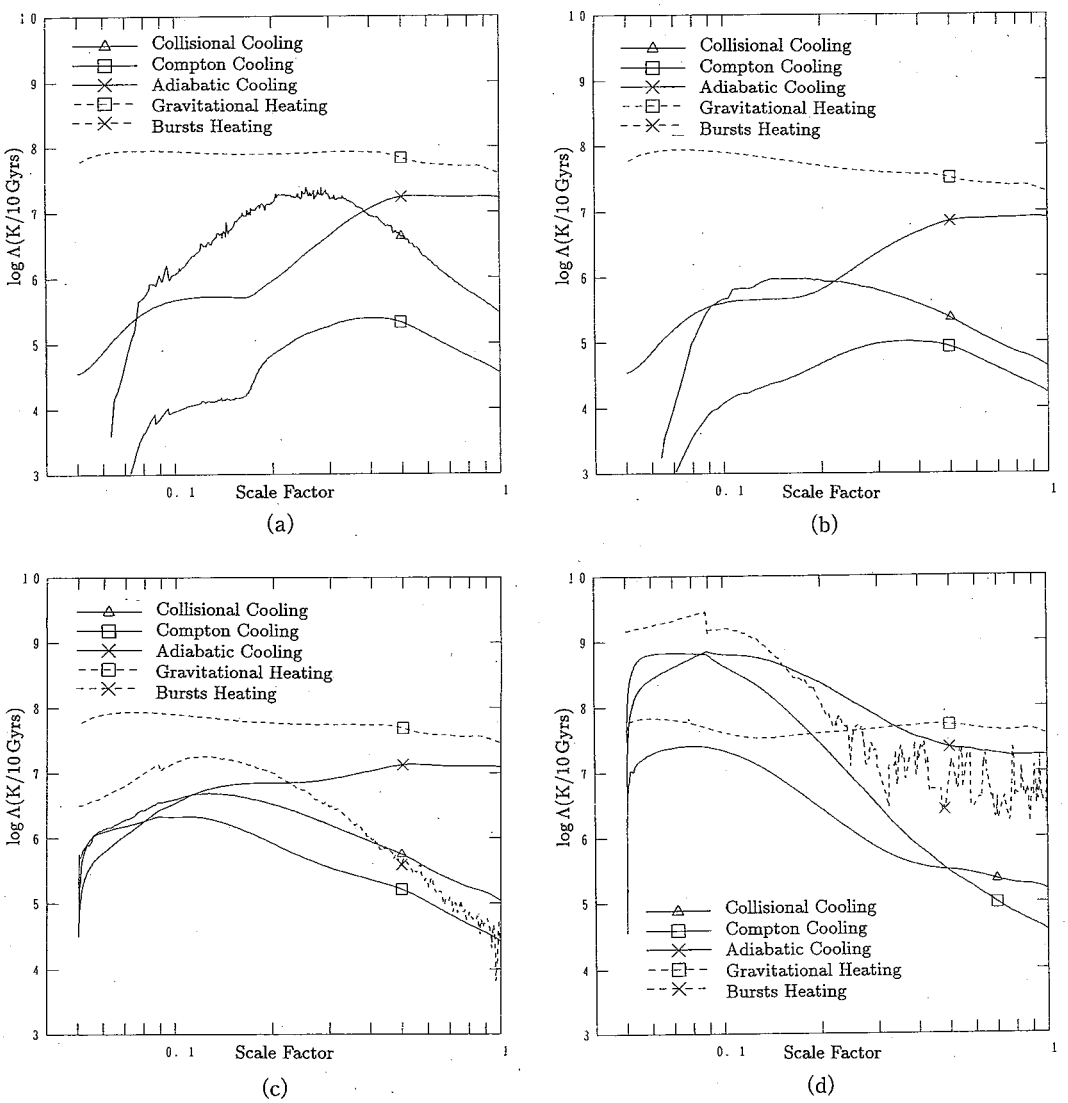

Fig. 2. The history of the rate of Compton cooling in $\Lambda_{\rm cool}$, the rate of line cooling, bremsstrahlung cooling, recombination cooling, dielectronic recombination cooling and ionization cooling in $\Lambda_{\rm cool}$, the rate of cooling by adiabatic expansion of the universe $-2\dot{a}/aE$, the rate of gravitational heating $-\rho_{\rm b}u_k/a\partial\phi/\partial x_k$, and the rate of heating by galactic bursts $\Lambda_{\rm heat}$. They are the spatially averaged values in units of Kelvin per 10 Gyrs. Correspondence of (a)~(d) is the same as in Fig. 1.

universe and the temperature increases above 10^5 K after $a\sim0.4$. Then the rate of "collisional" cooling becomes further small because it is not effective at temperature above 10^5 K. Since the rate of the adiabatic cooling is proportional to the temperature, it finally exceeds that of "collisional" cooling. The rate of Compton cooling is much smaller than that of the other cooling/heating processes.

For the model (B), the case that galaxies are formed but no galactic burst occurs, the density fluctuation of the IGM does not evolve apparently when $a<0.3$ since most of galaxies are formed at this epoch and the mass of dense cells is subtracted by

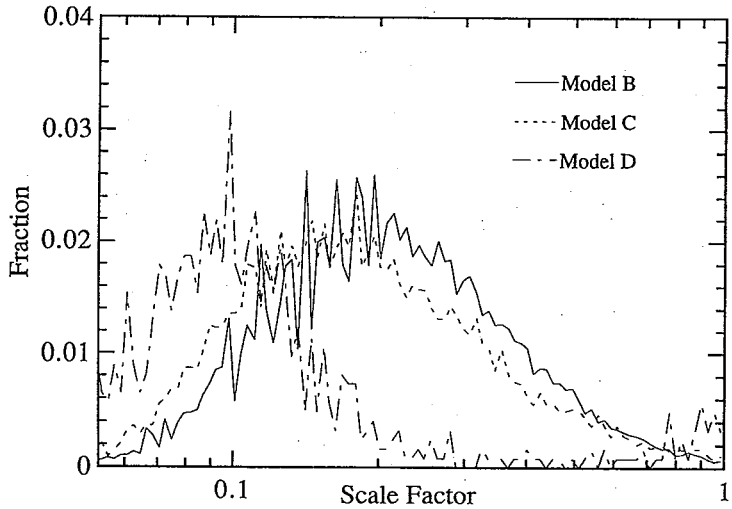

Fig. 3. The galaxy formation rate for the models (B)~(D). The rate is normalized by the total number of formed galaxies for each model.

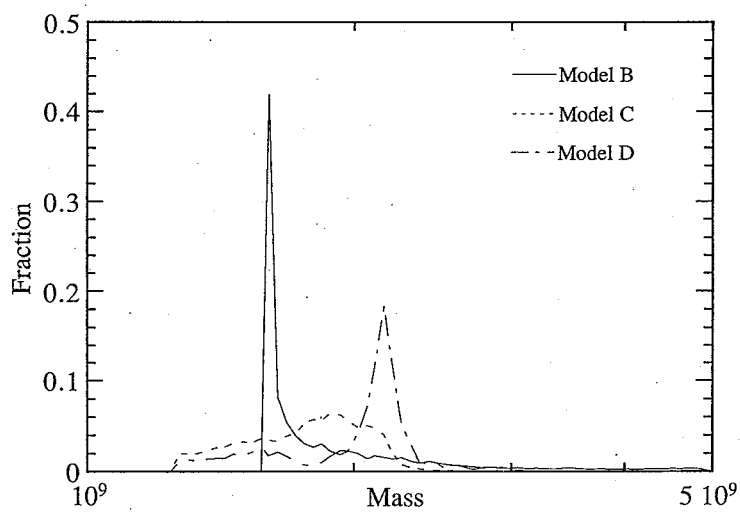

Fig. 4. Mass function of galaxies for the models (B)~(D). The normalization is the same as in Fig. 3.

formation of galaxies. Galaxies are not formed frequently after $a \sim 0.3$ and subtraction of the mass almost does not work at this time because the condition (v), $T < 2 \times 10^5$ K, is not satisfied at high density cells. Then the density fluctuation of IGM increases. The rate of "collisional" cooling for the model (B) is much lower than that for the model (A) due to subtraction of mass from high density cells. Therefore the temperature of IGM for the model (B) increases gradually but it does at earlier epoch than for the model (A).

As for the model (C), the case of forming galaxies with the emission parameter $\epsilon = 5 \times 10^{56}$, the density fluctuation of the IGM does not evolve when $a < 0.2$ and increases after $a \sim 0.2$ for the same reason as the model (B). The temperature rises

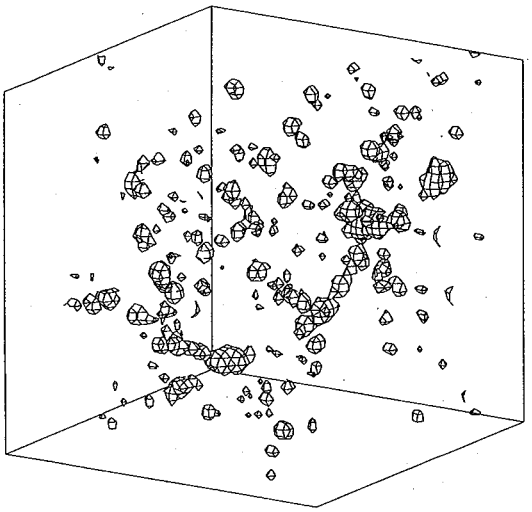

Fig. 5. Three dimensional plots of the density of the dark matter for the model (C) at present. The regions drawn correspond to $\rho \geq \langle\rho\rangle + 2\langle\delta\rho\rangle$.

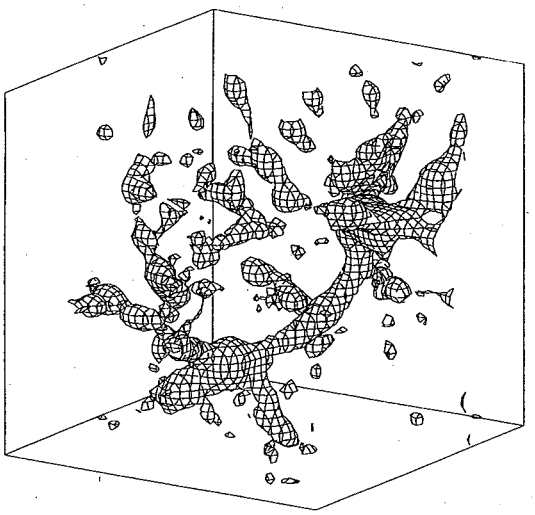

Fig. 6. Three dimensional plots of the density of the IGM for the model (C) at present. The regions drawn correspond to $\rho \geq \langle\rho\rangle + 2\langle\delta\rho\rangle$.

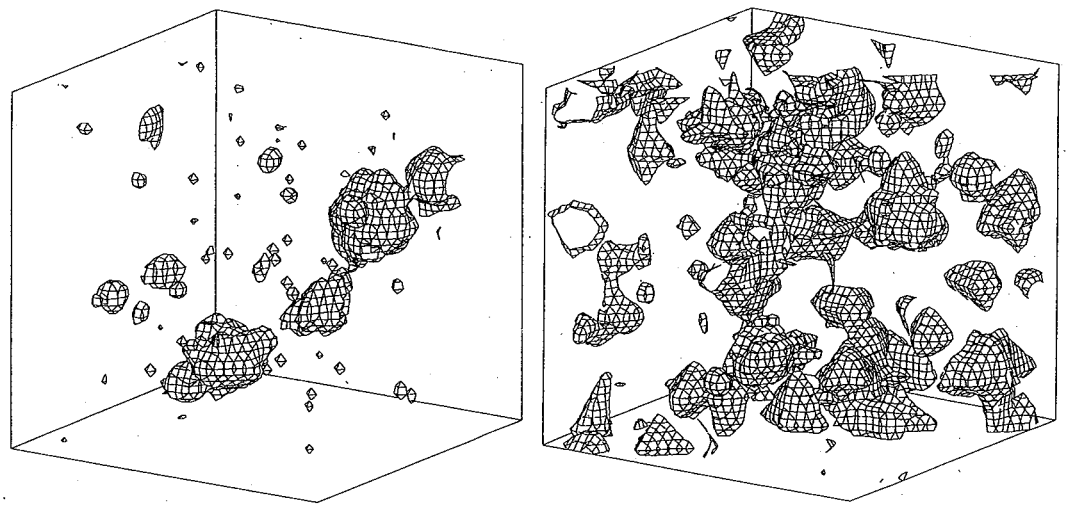

(a) (b)

Fig. 7. Three dimensional plots of the temperature of the IGM at present (a) for the model (C) and (b) for the model (D). The regions drawn correspond to $T \geq \langle T\rangle + 2\langle\delta T\rangle$ for the model (C) and $T \geq \langle T\rangle$ for the model (D).

above 10^5 K earlier than for the model (B) due to the galactic bursts, so the rate of galaxy formation is smaller and starts to decrease earlier. We note that the number of formed galaxies is 55011 for the model (B), 16359 for the model (C), and 1232 for the model (D), that finally the gaseous baryonic matter left in the IGM is 54% of baryon for the model (B), 77% for the model (C), and 98% for the model (D), and that the condition (v) almost prescribes this trend.

For the model (D), the case of forming galaxies and emitting a substantial energy,

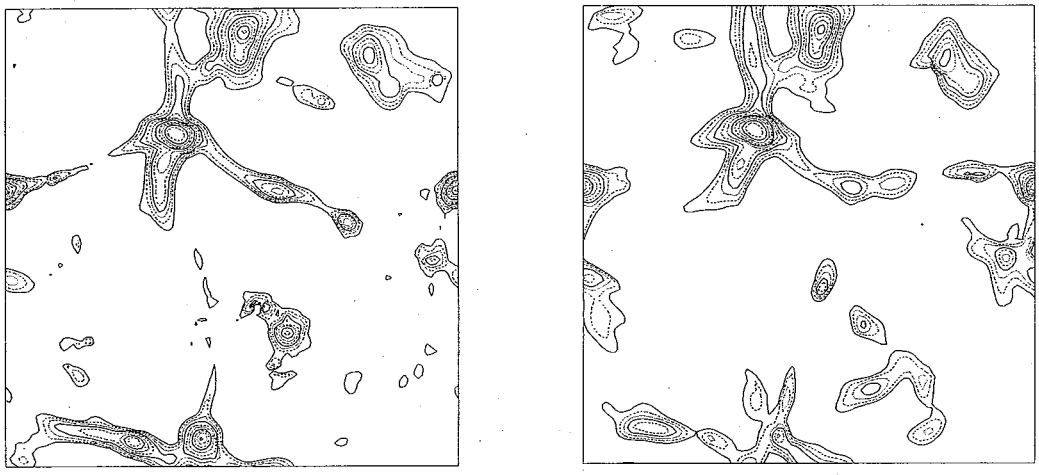

(a) (b)

Fig. 8. Contour plots of the density of the IGM at present (a) for the model (C) and (b) for the model (D). Thickness of a slice is one cell. The contour lines are $\rho_{\rm IGM}=1.4^n\langle\rho_{\rm IGM}\rangle$ with $n=0, 1, 2, \cdots, 10$. The contour levels increase as the solid line, the dashed line and the dotted line.

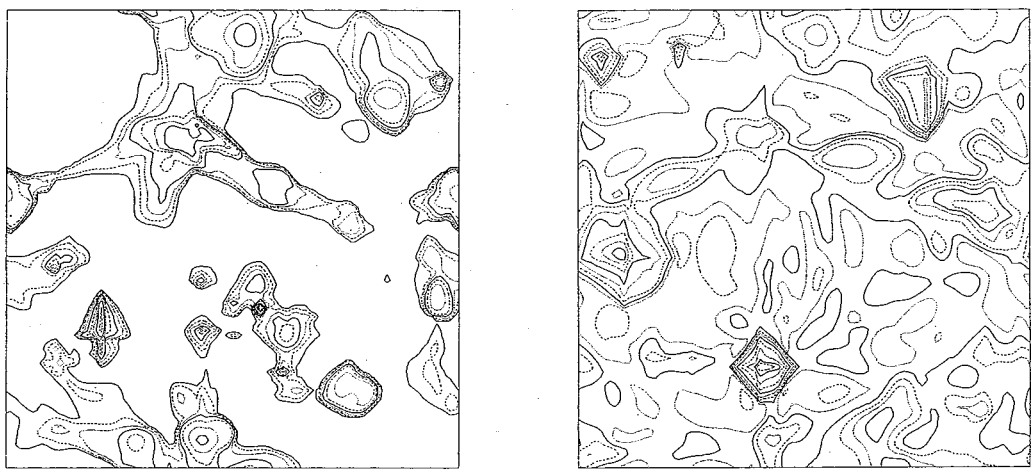

(a) (b)

Fig. 9. Contour plots of the temperature of the IGM at present (a) for the model (C) and (b) for the model (D). Thickness of a slice is one cell. The contour lines are $T=f^n\times10^5$ K with $n=0, 1, 2, \cdots, 10$ where $f=1.9$ for the model (C) and $f=2.2$ for the model (D). The contour levels increase as the solid line, the dashed line and the dotted line.

there is a curious feature in evolution of the density fluctuation of the IGM. The density fluctuation of the IGM grows a little faster than that of the dark matter when $a\lesssim0.1$ because of compression of the IGM by shock waves emitted from galaxies. It does not grow when $0.1\lesssim a\lesssim0.4$ because the thermal pressure is high especially at the high density regions. Formation of galaxies is gradually ceased due to the condition (v). Shock waves which are formed at $a\lesssim0.1$ propagate and cover the whole volume before $a\sim0.4$. Then the hot spots are not localized, which means that the tempera-

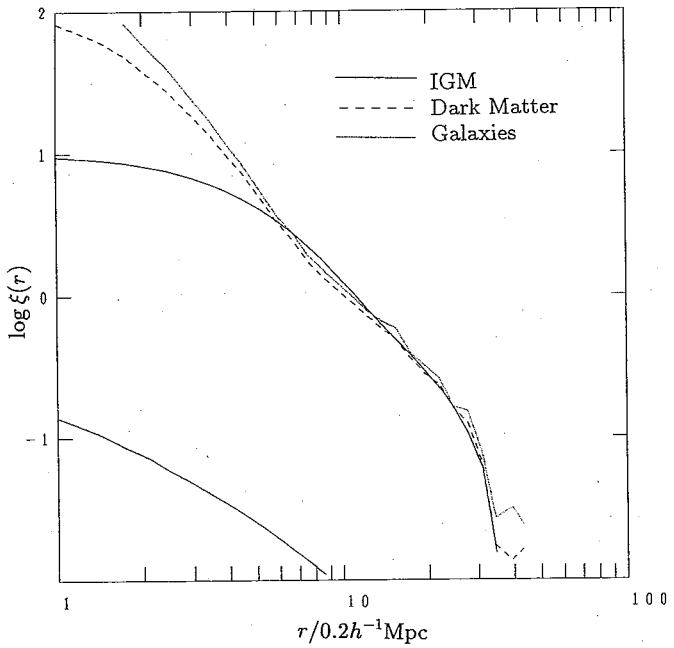

Fig. 10. Two point correlation function of the dark matter (dashed line), of the IGM (solid line), and of galaxies (dotted line) at present for the model (C). The bottom line is the two point correlation function of the dark matter and the IGM at initial time.

ture at the high density regions is not always higher than that at the low density regions, and the effect that the thermal pressure prevents the IGM from condensing becomes smaller. So the density fluctuation of the IGM grows again. We discuss the differences between Ryu et al.'s results[10] and ours in § 4.

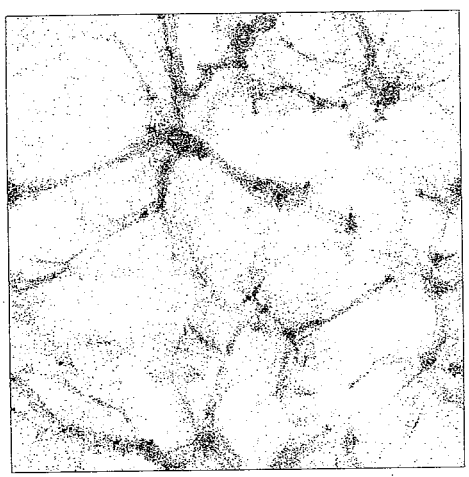

Fig. 11. Map of the location of the dark matter particles at present for the model (C). Thickness of a slice is 10 cells.

We show a mass function of galaxies in Fig. 4 for the models (B)~(D). Because the merging process and formation of galaxies made by cells more than eight are not taken into account, it should not be compared with observation such as the luminosity function. It provides whether the condition (iii), total mass criterion, is effective for galaxy formation. The curve of the mass function has a strong peak for the model (B) but the curves for the models (C) and (D) are flattened. So the condition (iii) strongly controls formation of galaxies for the model (B), but it seems less effective for the models (C) and (D), as seen in Fig. 4. The condition (v), the temperature criterion, plays an important role for the latter models since the regions which satisfy the condition (iii) have high temperature enough not

to satisfy the condition (v) at earlier epoch due to bursts.

The density fluctuation of the dark matter evolves in the same way for each model. This is because the dark matter couples to baryon only with gravity and its mass overwhelms mass of baryon.

3.2. *Distribution of IGM, galaxies and dark matter*

We present the 3-dimensional structures of the density of the dark matter and the IGM and the temperature of the IGM at present in Figs. 5~7. The 2-dimensional contour plots of the density of the IGM and the temperature of the IGM at present is shown in Figs. 8 and 9 for the models (C) and (D). We find that the structure of the density of the dark matter is not changed among the models for the reason described in the previous section and that the structure of the density of the IGM is also not changed much. The structure of the density of the IGM shows more largely connected feature than that of the dark matter, as seen in Figs. 5 and 6. This is because the thermal pressure is effective and the density of the IGM does not grow as well as

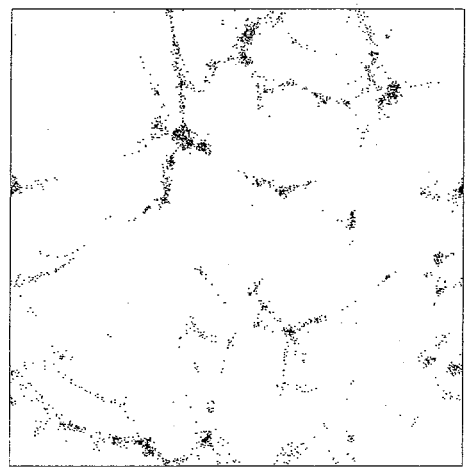

(a)

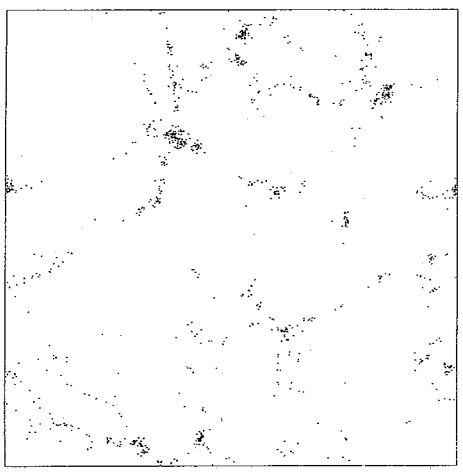

(b)

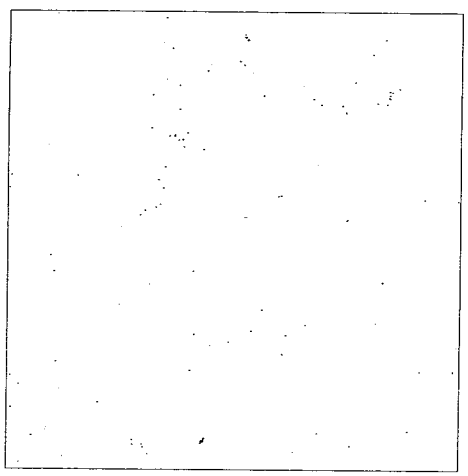

(c)

Fig. 12. Map of the location of the galactic particles at present (a) for the model (B), (b) for the model (C), and (c) for the model (D). Thickness of a slice is 10 cells.

that of the dark matter. This is more clearly shown in Fig. 10, which is the two point correlation function of the dark matter, the IGM, and galaxies at present. The condensation of the IGM is strongly suppressed on scales less than $2h^{-1}$ Mpc, as compared with the curve of the dark matter. The two point correlation function shows almost the same feature for all models. As for the distribution of galaxies, we find that the two point correlation function of galaxies gives a better fit to that of the dark matter than that of the IGM while its amplitude for galaxies is slightly larger than that for the dark matter due to the condition (iii), that is called biasing. The reason is as follows. Although galaxies behave as the IGM at epoch of its formation, their behavior approaches that of the dark matter with time since galaxies are treated as collisionless particles. In our models galaxies are formed early enough to forget properties of the IGM. Thus the property of the distribution of galaxies is similar to that of the dark matter. Galaxies lie at the high density regions of the dark matter, as seen in Figs. 11 and 12. This is mainly due to the condition (iii), which is strong enough to limit the regions where a galaxy can be formed.

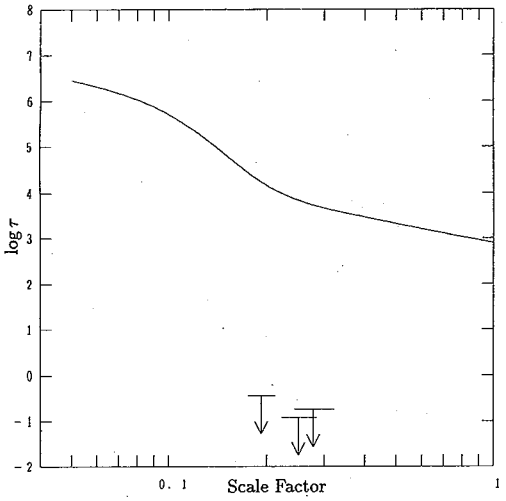

Fig. 13. The history of the optical depth of HI for the model (D). The arrows are the observed ones (Jenkins and Ostriker[4]).

We find from the three dimensional structure of the temperature at present, Fig. 7, that the high density regions are always the high temperature regions for the models (A)~(C). On the other hand for the model (D) the coincidence between the locations of high density and those of high temperature seems to be small. These are also clearly shown in Figs. 8 and 9. The hot spots for the models (A)~(C) are mainly heated by the energy released by gravity at high density regions. In the model (D) the regions heated by strong bursts out of young galaxies, whose energy overwhelms the energy released by gravity, are not localized but cover the whole volume. Then the high density regions forget having high temperature previously.

Although the mean temperature for all the models is finally greater than 10^5 K, all of the cells do not have temperature higher than 10^5 K. Therefore hydrogen cannot be fully ionized in the universe for our models and the optical depth of HI is much larger than unity, as seen in Fig. 13.

§ 4. Conclusions and discussion

We have presented the evolution and the distribution of the dark matter, the IGM, and galaxies by the three dimensional hydrodynamical numerical simulation. Cosmological expansion, self-gravity, cooling processes, galaxy formation, and galactic bursts are taken into account. Formation of galaxies is carried out when cubic neighboring eight cells satisfy five criteria related with Jeans mass, velocities, biasing

for total mass and mass of gas and temperature. We have considered four models, which are the case of no-formation of galaxies, the case of formation but no-burst, the case of formation with a reasonable amount of energy of bursts, and the case of formation with an extremely large amount of energy of bursts. Then the evolution and the distribution of the density and the temperature, and the history of cooling are calculated for each model. We have shown that these are complicatedly coupled to the criteria of galaxy formation and galactic bursts.

The "collisional" cooling is effective for $0.1 \lesssim a \lesssim 0.4$ and the Compton cooling is negligible for the models of no-strong bursts. On the other hand the Compton cooling is more effective than the "collisional" cooling for the model of the strongest bursts since the difference between the temperature of the IGM and that of photon is much larger.

As for the criteria of galaxy formation, the locations of galaxies are determined by the condition (iii) and the rate of galaxy formation is mainly controlled by the conditions (iii) and (v). The parameter α_1 determines the starting epoch of galaxy formation and the temperature condition affects the ending epoch of that. In particular for the model (D) the number of galaxies is much smaller than for the other models and the formation epoch is limited by $a \lesssim 0.2$, while continuing galaxy formation at present time is shown in Ryu et al.[10] Although the criteria are not studied here by changing their parameters, their effects on the evolution and the distribution of the IGM and galaxies may be large and the scenario we have shown above may be much changed. For example if we adopted $\alpha_1=0$, many galaxies would be formed at the places having nothing to do with the high density regions of the dark matter. In this analysis the effect of α_2 is not clarified.

As comparing our results with those in Cen and Ostriker,[13] we find they show essentially the same feature for the history of the IGM. So we confirm that our treatment of cooling and ionization is not inadequate. The difference in the epoch of galaxy formation between them is caused by the parameter of α_1. In order to explain the HI optical depth at $z \sim 4$ by an activity of young galaxies, the parameter of α_1 should be as small as the value which we adopt so that galaxies may be formed at early epoch.

As for the effects of bursts, we have found that there are not any strong differences in the thermal history and the distribution between model (B), $\epsilon=0$ and the model (C), $\epsilon=5\times10^{56}$. However the prediction of the model (D), $\epsilon=5\times10^{59}$ is quite different from that of the others. So we find that the critical energy to affect the structure on scales $\sim 1h^{-1}$ Mpc is 10^{57-59} erg since the energy of bursts is given by $\epsilon M/10^9\, M_\odot$ erg and the typical mass of a "galaxy" formed in this simulation is $10^9\, M_\odot$. Actually, the gravitational energy of the IGM in the box with scale length R is written as $GM_tM_{\rm IGM}/R \sim 10^{58}\ (R/1h^{-1}\ {\rm Mpc})^5 h^{-1} \rho_t \rho_{\rm IGM}/\rho_{\rm cr}{}^2$ erg.

The discrepancy between the predicted optical depth of HI and the observed ones is still a serious problem in the thermal history of the universe. The optical depth of HI in our calculations is significantly larger than the observed ones[4] even if the enormous energy input is given. On the other hand the optical depth in the simulation of Ryu et al.[10] is as small as the observed one. It may be due to the effect, in their calculations, that the energy of galactic bursts is too large and the temperature

criterion we adopted for galaxy formation is not included. Then much more galaxies are formed than for our model with the strongest bursts, the IGM is heated up too much, and the high temperature and the full degree of ionization are kept since galaxy formation and bursts continue even at the present epoch. It is unlikely that a young galaxy bursts the energy greater than its binding energy and also that a galaxy is formed after star formation occurs in a object with $T \gg 10^5$ K. Probably in order to reproduce the observed optical depth, it is necessary to introduce UV radiation. However Cen and Ostriker[13] show that it is still difficult to explain the small value of the observed HI optical depth when the UV radiation is taken into account in their calculations with the spatially averaged fashion. So it will be needed to perform the UV radiation in order to achieve full ionization of the IGM with non-spatially-averaged method and/or with galactic bursts of the UV band which is not included by them.

As seen above, a lot of physical processes including unknown parameters such as galactic bursts are related with the structure formation on scales less than $20h^{-1}$ Mpc. Therefore it is necessary to carry out a large number of simulations in order to determine the cosmological model and/or the galaxy formation model. An alternative study of the structure of the IGM on scales as large as $100h^{-1}$ Mpc might be useful for this purpose since the gaseous matter on such scales would not be suffered from complicated galactic properties so much. Then the observations of X-ray clusters at high redshift may give a key to solve the problem of the structure formation.

Acknowledgements

The author thanks H. Sato, N. Gouda, N. Sugiyama, M. Sasaki, Y. Yamada, Y. Suto and T. Matsuda for useful discussions, H. Kang and P. R. Shapiro for giving the cooling curve, and also thanks M. Den for reading this manuscript. Numerical computations were performed by FACOM VP-2600, FACOM M-780/30 and FACOM M-1800 at the Data Processing Center of Kyoto University.

References

1) V. de Lapparent, M. J. Geller and J. P. Huchra, Astrophys. J. Lett. **302** (1986), L1.
2) T. J. Broadhurst, R. S. Ellis, D. C. Koo and A. S. Koo, Nature **343** (1990), 726.
3) J. E. Gunn and B. A. Peterson, Astrophys. J. **142** (1965), 1633.
4) E. B. Jenkins and J. P. Ostriker, Astrophys. J. **376** (1991), 33.
5) S. D. M. White, C. S. Frenk, M. Davis and G. Efstathiou, Astrophys. J. **313** (1987), 505.
6) S. D. M. White, M. Davis, G. Efstathiou and C. S. Frenk, Nature **330** (1987), 451.
7) R. G. Carlberg, Astrophys. J. **324** (1988), 664.
8) M. J. West, J. V. Villumsen and A. Dekel, Astrophys. J. **369** (1991), 287.
9) W. H. Chiang, D. Ryu and E. T. Vishniac, Astrophys. J. **339** (1989), 603.
10) D. Ryu, E. T. Vishniac and W. H. Chiang, Astrophys. J. **354** (1990), 389.
11) R. Y. Cen, A. Jameson, F. Liu and J. P. Ostriker, Astrophys. J. Lett. **362** (1990), L41.
12) R. Y. Cen, Astrophys. J. Suppl. **78** (1992), 341.
13) R. Cen and J. Ostriker, Astrophys. J. **393** (1992), 22.
14) M. Saito, Publ. Astron. Soc. Jpn. **31** (1979), 181.
15) G. Efstathiou, M. Davis, C. S. Frenk and S. D. M. White, Astrophys. J. Suppl. **57** (1985), 241.
16) T. Matsuda, private communications.
17) H. Kang and P. R. Shapiro, private communications.
18) J. M. Bardeen, J. R. Bond, M. Kaiser and A. S. Szalay, Astrophys. J. **304** (1986), 15.